The Journal of Fourier Analysis and Applications

Volume 10, Issue 1, 2004

Wavelets Based on Prolate Spheroidal Wave Functions

Gilbert G. Walter and Xiaoping Shen

Communicated by Yang Wang

ABSTRACT. The article is concerned with a particular multiresolution analysis (MRA) composed of Paley–Wiener spaces. Their usual wavelet basis consisting of sinc functions is replaced by one based on prolate spheroidal wave functions (PSWFs) which have much better time localization than the sinc function. The new wavelets preserve the high energy concentration in both the time and frequency domain inherited from PSWFs. Since the size of the energy concentration interval of PSWFs is one of the most important parameters in some applications, we modify the wavelets at different scales to retain a constant energy concentration interval. This requires a slight modification of the dilation relations, but leads to locally positive kernels. Convergence and other related properties, such as Gibbs phenomenon, of the associated approximations are discussed. A computationally friendly sampling technique is exploited to calculate the expansion coefficients. Several numerical examples are provided to illustrate the theory.

1. Introduction

The continuous *prolate spheroidal wave functions* (PSWFs) are those that are most highly localized simultaneously in both the time and frequency domain (in a sense given later). This fact was discovered by Slepian and his collaborators and was presented in a series of articles [9], [10], [17]–[19] about forty years ago. Since then the study of PSWFs has been an active area of research in both electrical engineering and mathematics.

Although PSWFs had been shown to be the best tools for analyzing some problems raised in signal processing and telecommunication (Jain [7]), they are still often regarded as mysterious and are seldom used in practice. Historically, this was due partly to the limitations of machine computation. However, modern computational facilities and the recently developed numerical algorithms of Beylkin and Monzon [1] and of Xiao, Rokhlin and Yarvin [26] promise to provide elegant numerical results with satisfactory complexity.

Math Subject Classifications. 42A10, 42A15, 42C40.
Keywords and Phrases. Prolate spheroidal wave function, sampling, Paley–Wiener space, bandlimited signal, wavelets, Gibbs phenomenon.

ISSN 1069-5869

Today, PSWFs can be expected to become a versatile and powerful analysis tool and make more of an impact in engineering practice.

In this article, we discuss multiscale properties of these PSWFs and then construct systems which inherit the high energy concentration property of PSWFs and possesses a multiscale structure similar to wavelet families. One of the systems will be composed of true wavelet scaling functions, while the other will involve a modification to keep the concentration interval fixed at different scales.

To begin with, we recall the connection between PSWFs and the Shannon sampling theorem (Shannon [16]) given by the formula

$$f(t) = \sum_{n=-\infty}^{\infty} f(n) \frac{\sin \pi(t-n)}{\pi(t-n)} \ . \tag{1.1}$$

It holds for π- bandlimited signals with finite energy, that is, for continuous functions in $L^2(R)$ whose Fourier transform has support in $[-\pi, \pi]$. This theorem has become a well-known part of both the mathematical and engineering literature (see the recent books by Higgins [5] and Zayed [27] or the article by Vaidyanathan [20]).

The sinc function $S(t) = \frac{\sin \pi t}{\pi t}$ which appears in this formula is closely related to the PSWFs $\varphi_{n,\sigma,\tau}(t)$. They constitute an orthonormal basis of the space of $\sigma-$ bandlimited functions on the real line. They are concentrated on the interval $[-\tau, \tau]$ and, of course, depend on the two parameters σ and τ. There are several ways of characterizing them:

- as the eigenfunctions of an integral operator:

$$\frac{\sigma}{\pi} \int_{-\tau}^{\tau} \varphi_{n,\sigma,\tau}(x) S\left(\frac{\sigma}{\pi}(t-x)\right) dx = \lambda_{n,\sigma,\tau} \varphi_{n,\sigma,\tau}(t) \ . \tag{1.2}$$

- as the eigenfunctions of a differential operator:

$$\left(\tau^2 - t^2\right) \frac{d^2 \varphi_{n,\sigma,\tau}}{dt^2} - 2t \frac{d\varphi_{n,\sigma,\tau}}{dt} - \sigma^2 t^2 \varphi_{n,\sigma,\tau} = \mu_{n,\sigma,\tau} \varphi_{n,\sigma,\tau} \ . \tag{1.3}$$

  or

- as the maximum energy concentration of a $\sigma-$ bandlimited function on the interval $[-\tau, \tau]$; that is $\varphi_{0,\sigma,\tau}$ is the function of total energy 1 $(= ||\varphi_{0,\sigma,\tau}||^2)$ such that

$$\int_{-\tau}^{\tau} |f(t)|^2 \, dt$$

  is maximized, $\varphi_{1,\sigma,\tau}$ is the function with the maximum energy concentration among those functions orthogonal to $\varphi_{0,\sigma,\tau}$, etc.

Still another characterization in terms of multiplication operators is possible and may be found in Walter [22], while another integral eigenvalue problem also satisfied by the $\varphi_{n,\sigma,\tau}$ is (Papoulis [14])

$$\int_{-\tau}^{\tau} \varphi_{n,\sigma,\tau}(x) e^{i\sigma\omega x/\tau} \, dx = \gamma_{n,\sigma,\tau} \varphi_{n,\sigma,\tau}(\omega) \ . \tag{1.4}$$

The parameter τ comes from the interval of concentration and the parameter σ comes from the support of the Fourier transform . We can remove one of these parameters by changing the scale, and therefore can restrict our discussion to the $\pi-$ bandlimited case,

or alternately, to the concentration interval $[-1, 1]$. Both standardizations are used; the former for discrete sampling and the latter for calculations. Figure 1 shows several of the PSWFs on the concentration interval $[-1, 1]$.

We shall be interested mainly in $\varphi_{0,\sigma,\tau}$, the PSWF with maximum concentration on the given interval. It will be used to construct a scaling function and hence to obtain a basis composed of its translates. A multiresolution analysis and a mother wavelet are then based on this construction. Since in general, $\varphi_{k,\sigma,\tau}$ has exactly k zeros in the interval $[-\tau, \tau]$, in particular $\varphi_{0,\sigma,\tau}$ is strictly greater than zero in this concentration interval (but has an infinite number of zeros outside of the interval). Outside of the concentration interval, it can be made arbitrarily small if either τ or σ is made sufficiently large. These remarkable properties will be used in several occasions later on.

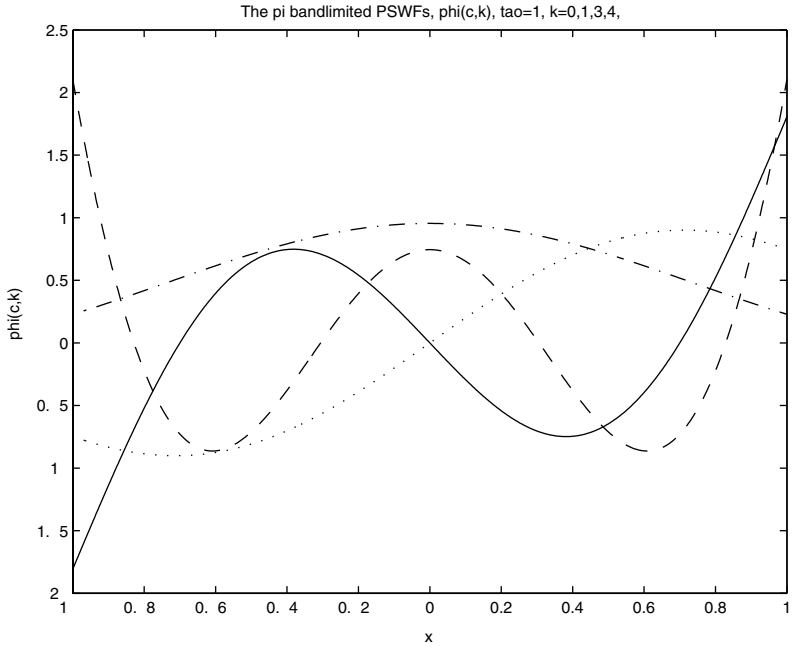

FIGURE 1 The π- bandlimited PSWFs (normalized by $||\varphi_{n,\pi,1}||_{L_2} = 1$), $\varphi_{k,\pi,1}(t)$, $k = 0$ (dot-dashed), 1 (dotted), 3 (solid), 4 (dashed), on interval $[-1, 1]$.

We conclude this introduction by giving the outline of this article as the follows: A brief review of some related properties of PSWFs will be given in the next section. By using these properties, we are able to introduce a new class of scaling functions and wavelets based on two different approaches in Section 3. This is followed by discussions of some properties related to convergence when these PSWFs are used for approximations as part of a multiscale system. Sampling properties (Walter and Shen [23] and [24]) are then exploited to calculate the expansion series. Finally, in the last section, some numerical examples are used to illustrate the theoretical results presented. A remark about further study is given at the close of the article.

2. Properties of Prolate Spheroidal Wave Functions

To refresh our memory, we recall some properties of PSWFs. These formulae are quite well known and are often easy to show. They may be found in a number of places (Landau [11], Landau and Pollak [9, 10], Landau and Widom [8], Papoulis [14], Slepian [18, 19], Slepian and Pollak [17]).

a. The dual orthogonality

In addition to the Equation (1.2), the $\{\varphi_{n,\sigma,\tau}\}$ satisfy an integral equation over $(-\infty, \infty)$ as well:

$$\int_{-\infty}^{\infty} \varphi_{n,\sigma,\tau}(x) S_\sigma(t-x)\,dx = (\varphi_{n,\sigma,\tau} * S_\sigma)(t) = \varphi_{n,\sigma,\tau}(t) \tag{2.1}$$

where $S_\sigma(t) = \frac{\sigma}{\pi} S(\frac{\sigma t}{\pi})$.

This leads to a dual orthogonality

$$\begin{aligned} \int_{-\tau}^{\tau} \varphi_{n,\sigma,\tau}(x)\varphi_{m,\sigma,\tau}(x)\,dx &= \lambda_{n,\sigma,\tau}\delta_{nm}\,, \\ \int_{-\infty}^{\infty} \varphi_{n,\sigma,\tau}(x)\varphi_{m,\sigma,\tau}(x)\,dx &= \delta_{nm} \end{aligned} \tag{2.2}$$

and the fact that they constitute an orthogonal basis of $L^2(-\tau, \tau)$, as well as an orthornormal basis of the subspace B_σ of $L^2(-\infty, \infty)$, the Paley–Wiener space of all $\sigma-$bandlimited functions.

b. The Fourier transforms

As one might expect, PSWFs are closely related to the Fourier transforms. Indeed, the Fourier transform of $\varphi_{n,\sigma,\tau}$ is given by

$$\widehat{\varphi}_{n,\sigma,\tau}(\omega) = (-1)^n \sqrt{\frac{2\pi\tau}{\sigma\lambda_{n,\sigma,\tau}}} \varphi_{n,\sigma,\tau}\left(\frac{\tau\omega}{\sigma}\right) \chi_\sigma(\omega) \tag{2.3}$$

where $\chi_\sigma(\omega)$ is the characteristic function of $[-\sigma, \sigma)$. Therefore the inverse Fourier transform gives us still another formula:

$$\varphi_{n,\sigma,\tau}(t) = (-1)^n \sqrt{\frac{2\pi\tau}{\sigma\lambda_{n,\sigma,\tau}}} \frac{1}{2\sigma} \int_{-\sigma}^{\sigma} \varphi_{n,\sigma,\tau}\left(\frac{\tau\omega}{\sigma}\right) e^{i\omega t}\,d\omega\,.$$

By a change of variable, this becomes (1.4).

A Fourier transform pair of the PSWF $\varphi_{n,\sigma,\tau}$ is shown in Figure 2.

The Fourier transform is also used to construct other formulae which will be useful to us later. For instance, the PSWFs shifted by integers can be used to construct a partition

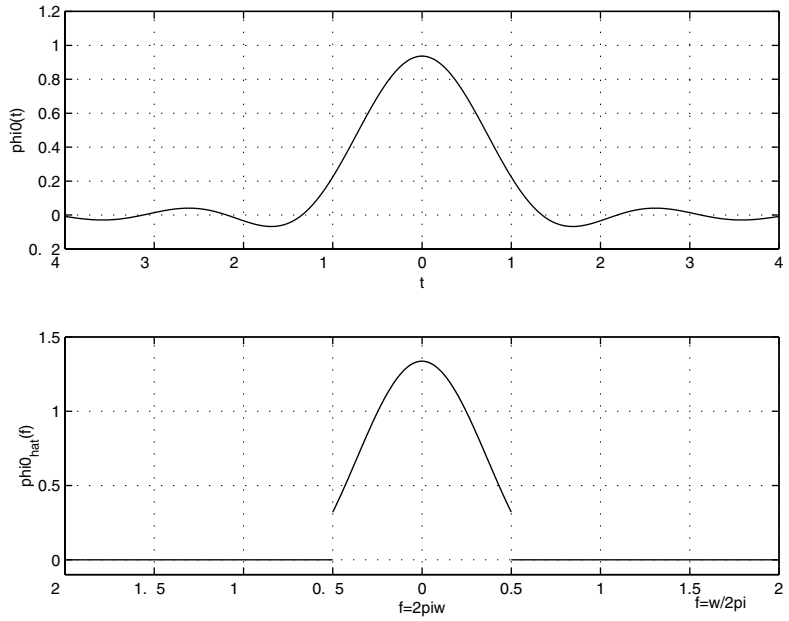

FIGURE 2 A Fourier pair of $\pi-$ bandlimited PSWF $\varphi_{0,\pi,\tau}$ and $\widehat{\varphi}_{0,\pi,\tau}$, $\tau = 1$.

of unity since

$$\begin{aligned}
\sum_{k=-\infty}^{\infty} \varphi_{n,\sigma,\tau}\left(t-\frac{k\pi}{\sigma}\right) &= \sum_{k=-\infty}^{\infty} \int_{-\infty}^{\infty} \varphi_{n,\sigma,\tau}(x) S_\sigma\left(t-x-\frac{k\pi}{\sigma}\right) dx \\
&= \int_{-\infty}^{\infty} \varphi_{n,\sigma,\tau}(x) \sum_{k=-\infty}^{\infty} S_\sigma\left(t-x-\frac{k\pi}{\sigma}\right) dx \\
&= \frac{\sigma}{\pi} \int_{-\infty}^{\infty} \varphi_{n,\sigma,\tau}(x)\, dx \\
&= \frac{\sigma}{\pi} \widehat{\varphi}_{n,\sigma,\tau}(0) \\
&= (-1)^n \sqrt{\frac{2\sigma\tau}{\pi\lambda_{n,\sigma,\tau}}} \varphi_{n,\sigma,\tau}(0)\ .
\end{aligned}$$

This may be rewritten for $n = 0$, as

$$\frac{1}{\varphi_{0,\sigma,\tau}(0)} \sqrt{\frac{\pi\lambda_{0,\sigma,\tau}}{2\sigma\tau}} \sum_{k=-\infty}^{\infty} \varphi_{0,\sigma,\tau}\left(t-\frac{k\pi}{\sigma}\right) = 1 \tag{2.4}$$

i.e., we get a partition of unity.

c. The associated eigenvalues

The eigenvalues $\lambda_{n,\sigma,\tau}$ that appear above have a number of interesting properties. They are positive and non-increasing, i.e., satisfy $\lambda_{0,\sigma,\tau} \geq \lambda_{1,\sigma,\tau} \geq \lambda_{2,\sigma,\tau} \geq \ldots > 0$, and, in fact, the first $[\sigma\tau]$ are relatively close to 1 while the remaining ones are decreasing very rapidly to 0 as shown in Figure 3 below (see Slepian [19] for more details).

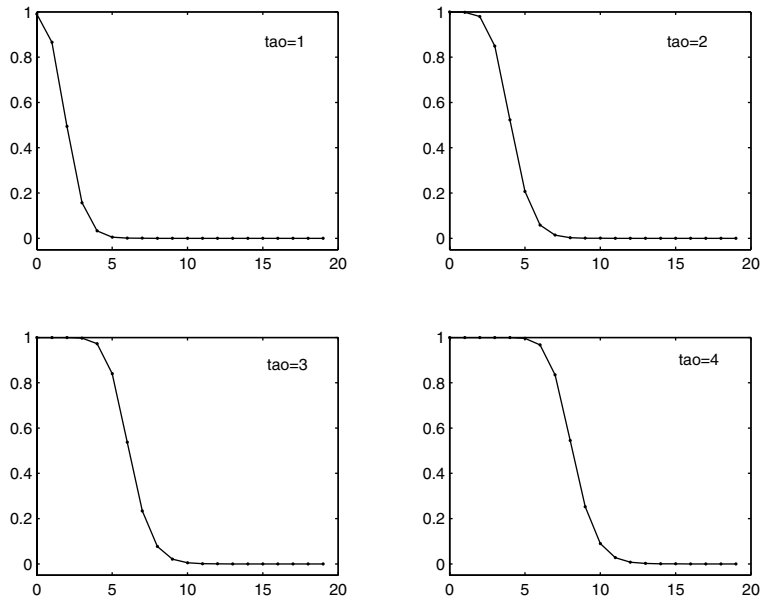

FIGURE 3 The "Step function" property of eigenvalues of $\pi-$ bandlimited PSWFs, $\tau = 1, 2, 3,$ and 4.

d. Multiscale structure

It is possible to find the relation between these functions at different scales by using the above definitions and formulas. By a straightforward change of scale in the integral Equation (1.2), we find that

$$\varphi_{n,\sigma\tau,1}(x) = \sqrt{\tau}\ \varphi_{n,\sigma,\tau}(\tau x)\ . \tag{2.5}$$

Then (2.5) leads to the following relation between scales

$$\varphi_{0,\sigma,\tau}(x) = \sqrt{1/a}\ \varphi_{0,a\sigma,\tau/a}(x/a) \tag{2.6}$$

for any $a > 0$. In particular for $a = 2$, we have

$$\sqrt{2}\ \varphi_{0,\sigma,\tau}(2x) = \varphi_{0,2\sigma,\tau/2}(x)\ . \tag{2.7}$$

Remark 1. There are two ways in which the PSWFs are usually standardized. One is to adjust the frequency so that $\varphi_{n,\sigma,\tau}$ becomes $\pi-$ bandlimited. The other is to adjust the time so that the concentration interval is $(-1, 1)$. Either one but not both can be attained by a change of scale as in (2.7). Indeed we have that

$$\varphi_{0,\sigma,\tau}(x) = \sqrt{\sigma/\pi}\ \varphi_{0,\pi,\tau\sigma/\pi}(\sigma x/\pi) = \sqrt{1/\tau}\ \varphi_{0,\tau\sigma,1}(x/\tau)\ .$$

3. Prolate Spheroidal Wavelets

In order to construct these PSWF wavelets, we begin with a scaling function ϕ, whose integer translates are a Riesz basis of a space V_0. This space is usually taken to be a subspace of $L^2(\mathbb{R})$. In our case we shall take $\phi(x) = \varphi_{0,\pi,\tau}(x)$, where τ is any positive

number. With this choice the space V_0 will turn out to be the Paley–Wiener space B_π of $\pi-$ bandlimited functions no matter what the choice of τ.

This space then becomes part of a family of nested subspaces usually referred as a multiresolution analysis (MRA). The other spaces are obtained by dilations by factors of two: $f(t) \in V_m$ if and only if $f(2^{-m}t) \in V_0$. These have the usual properties of an MRA:

(i) $\cdots \subseteq V_{m-1} \subseteq V_m \subseteq \cdots \subseteq L^2(\mathbb{R})$,
(ii) $\overline{\cup V_m} = L^2(\mathbb{R})$,
(iii) $\cap V_m = \{0\}$.

The MRA consisting of the Paley–Wiener spaces ($V_m = B_{2^m\pi}$) has been widely studied and has as its standard scaling function the sinc function $S(t) = \sin \pi t/\pi t$ mentioned in the introduction. This function has very good frequency localization, but not very good time localization (in fact is not even in $L^1(\mathbb{R})$). This has limited its use as a wavelet basis in comparison to the Daubechies wavelets which have compact support in the time domain. Because of the properties of entire functions, no bandlimited function has compact support in the time domain. However the PSWF's are as close to it as one can get, and in fact, for τ sufficiently large, can be made arbitrarily small outside of the interval of concentration. Hence they should be similar to the Daubechies wavelets for practical computations and superior to the sinc functions.

We borrow a number of techniques from wavelet theory to obtain a new basis for V_0 (see Daubechies [3, p. 140] and Walter and Shen [25, p. 40, 189]). This will differ from the standard wavelet basis for V_0 consisting of translates of the sinc function.

Proposition 1.

A bounded function $\theta(t)$ in $L^1(\mathbb{R})$ with unit norm in $L^2(\mathbb{R})$
(i) *is a Riesz basis of its closed linear span in $L^2(\mathbb{R})$ if and only if*

$$0 < A \leq \sum_{k=-\infty}^{\infty} \left|\widehat{\theta}(\omega - 2\pi k)\right|^2 \leq B < \infty\,, \tag{3.1}$$

(ii) *is orthogonal to its integer translates if and only if*

$$\sum_{k=-\infty}^{\infty} \left|\widehat{\theta}(\omega - 2\pi k)\right|^2 = 1\,, \tag{3.2}$$

(iii) *is a sampling function if it is a Riesz basis and*

$$\sum_{k=-\infty}^{\infty} \widehat{\theta}(\omega - 2\pi k) = 1\,. \tag{3.3}$$

Since both $\varphi_{0,\pi,\tau}(x)$ and $\widehat{\varphi}_{0,\pi,\tau}(\omega)$ are PSWF's locally at least, we may use either one to obtain a basis of a space V_0. However we are interested mainly in finding a new basis of the Paley Wiener spaces and therefore shall consider only the former.

3.1 PS Wavelets in Paley–Wiener Space

In order to obtain a Riesz basis based on PSWFs in the space B_π we must show that translates of $\widehat{\varphi}_{0,\pi,\tau}$ satisfy (3.1). The calculations are not too difficult and give us:

Proposition 2.

Let $\varphi_{0,\pi,\tau}(t)$ be a $\pi-$bandlimited PSWF with concentration interval $[-\tau, \tau]$; then
(i) $\{\varphi_{0,\pi,\tau}(t-n)\}$ *is a Riesz basis of B_π and*
(ii) $\zeta_{0,\pi,\tau}(t)$ *given by*

$$\widehat{\zeta}_{0,\pi,\tau}(\omega) := \widehat{\varphi}_{0,\pi,\tau}(\omega)/\widehat{\varphi^*}_{0,\pi,\tau}(\omega)\ ,$$

where $\sum_{k=-\infty}^{\infty} \widehat{\varphi}_{0,\pi,\tau}(\omega - 2\pi k) = \widehat{\varphi^*}_{0,\pi,\tau}(\omega)$, is a sampling function. That is, for each $f \in B_\pi$,

$$f(t) = \sum_{n=-\infty}^{\infty} f(n)\zeta_{0,\pi,\tau}(t-n)\ .$$

For the proof, we first observe that $\varphi_{0,\pi,\tau}(t)$ has no zeros in the interval $[-\tau, \tau]$ (see Slepian [19]). Now we take the periodic extension of $|\widehat{\varphi}_{0,\pi,\tau}(\omega)|^2$ with the convention that $\chi_\pi(t)$ be the characteristic function of $[-\pi, \pi)$. This gives us:

$$\begin{aligned}
&\sum_{k=-\infty}^{\infty} \left|\widehat{\varphi}_{0,\pi,\tau}(\omega - 2\pi k)\right|^2 \qquad (3.4)\\
&= \frac{2\tau}{\lambda_{0,\pi,\tau}} \sum_{k=-\infty}^{\infty} |\varphi_{0,\pi,\tau}((\omega - 2\pi k)\tau/\pi)|^2 \chi_\pi(\omega - 2\pi k)\\
&\geq \inf_{|\omega|\leq\pi} \frac{2\tau}{\lambda_{0,\pi,\tau}} |\varphi_{0,\pi,\tau}(\omega\tau/\pi)|^2 > 0
\end{aligned}$$

by (2.3). Similarly we see that

$$\sum_{k=-\infty}^{\infty} \left|\widehat{\varphi}_{0,\pi,\tau}(\omega - 2\pi k)\right|^2 \leq \sup_{|\omega|\leq\pi} \frac{2\tau}{\lambda_{0,\pi,\tau}} |\varphi_{0,\pi,\tau}(\omega\tau/\pi)|^2 < \infty\ . \qquad (3.5)$$

Thus we may conclude that $\{\varphi_{0,\pi,\tau}(t-n)\}$ is a Riesz basis of its closed linear span by Proposition 1 (i)

This closed linear span is, in fact, B_π, the Paley–Wiener space. This follows from the fact that any element of this space is a function f in $L^2(\mathbb{R})$ whose Fourier transform has support in $[-\pi, \pi]$. Thus $\widehat{f}/\widehat{\varphi}_{0,\pi,\tau}$ may be expanded in a Fourier series on $[-\pi, \pi]$ convergent in the sense of L^2 on this interval since $\widehat{\varphi}_{0,\pi,\tau}$ has no zeros in $[-\pi, \pi]$ and is continuous there. Hence $\widehat{f}$ has an L^2 convergent series of the form

$$\sum_{n=-\infty}^{\infty} a_n \widehat{\varphi}_{0,\pi,\tau}(\omega) e^{-i\omega n}\ .$$

Then by taking the inverse Fourier transform we get a series in $\sum_{n=-\infty}^{\infty} a_n \varphi_{0,\pi,\tau}(t-n)$ convergent to the inverse Fourier transform of f which is an element of B_π.

We now need only to show that $\zeta_{0,\pi,\tau}(t)$ is a sampling function which we do by using (3.3) for its construction. It is again a $\pi-$ bandlimited function since $\widehat{\varphi^*}_{0,\pi,\tau}(\omega)$ is the periodic extension of a function which is positive on $[-\pi, \pi)$. The last conclusion follows from the fact that $\{\zeta_{0,\pi,\tau}(t-n)\}$ is also a Riesz basis by the same argument as before. (In fact, the astute observer will notice that this is exactly the Shannon sampling theorem.)

Thus $\varphi_{0,\pi,\tau}$ is a candidate for a scaling function with $V_0 = B_\pi$. There are several ways of constructing bases of the other subspaces $V_m = B_{2^m\pi}$ from those of V_0. One uses the standard wavelet approach in which dilations of $\varphi_{0,\pi,\tau}$, i.e., $\varphi_{0,\pi,\tau}(2^m t)$ are used to get the basis $\{\varphi_{0,\pi,\tau}(2^m t - n)\}$ of V_m. In this case we get

$$\phi\left(2^m t\right) = \varphi_{0,\pi,\tau}\left(2^m t\right) = 2^{m/2}\varphi_{0,2^m\pi,2^{-m}\tau}(t)\ ,$$

i.e., the concentration interval becomes progressively smaller as m increases. The size of the concentration interval and band limited level, are in fact, the most important properties that distinguish the PSWF system. In order to avoid losing these properties, we have to find a way to make sure the concentration interval remains constant. We may do this by taking $\{\varphi_{0,2^m\pi,\tau}(t - n2^{-m})\}$ instead as a possible Riesz basis of V_m. That it is follows from the same calculations as in Proposition 2.

It is also possible to find a dual Riesz basis for $\{\varphi_{0,\pi,\tau}(t - n)\}$. We can get it by a slight extension of the results in Proposition 1, namely by defining the Fourier transform of the dual function $\widetilde{\varphi}_{0,\pi,\tau}(t)$ as

$$\widehat{\widetilde{\varphi}}_{0,\pi,\tau}(\omega) := \frac{\widehat{\varphi}_{0,\pi,\tau}(\omega)}{\sum_k \left|\widehat{\varphi}_{0,\pi,\tau}(\omega - 2\pi k)\right|^2}\ . \tag{3.6}$$

From this it follows that

$$\sum_k \widehat{\widetilde{\varphi}}_{0,\pi,\tau}(\omega - 2\pi k)\overline{\widehat{\varphi}_{0,\pi,\tau}(\omega - 2\pi k)} = 1$$

and by the extension just mentioned, that $\{\widetilde{\varphi}_{0,\pi,\tau}(t - n)\}$ is biorthogonal to $\{\varphi_{0,\pi,\tau}(t - n)\}$. Again, because $\widehat{\widetilde{\varphi}}_{0,\pi,\tau}(\omega)$ is positive on $[-\pi, \pi]$, it follows that $\{\widetilde{\varphi}_{0,\pi,\tau}(t - n)\}$ is a Riesz basis of B_π.

3.2 Dilation Equations

The dilation equations give the relation between the bases of V_m and V_{m+1}.

For $m = 0$, the dilation equation is given in the form

$$\phi_0(t) = \sum_k c_k^0 \phi_1(t - k/2) \tag{3.7}$$

where $\phi_0(t) = \varphi_{0,\pi,\tau}(t)$ and either $\phi_1(t) = \varphi_{0,2\pi,\tau}(t)$ (our modified scaling function in V_1) or $\phi_1(t) = \sqrt{2}\varphi_{0,\pi,\tau}(2t)$ (the standard scaling function in V_1). Of course the coefficients would also be different in the two cases.

The standard wavelet approach leads us to the same dilation equation at each scale; however, it also winds up with shrinking concentrations in the time domain as we have noted. The alternate approach, which is the one we concentrate on mostly hereafter, has the advantage of keeping the size of concentration interval constant with the only difference being that the dilation equations are slightly different at different scales.

The Fourier transformed version of (3.7) is

$$\begin{aligned}\widehat{\varphi}_{0,\pi,\tau}(\omega) &= \sum_k \frac{1}{\sqrt{2}} c_k^0 e^{-ik\omega/2}\widehat{\varphi}_{0,\pi,\tau}(\omega/2) \\ &= \frac{1}{\sqrt{2}} m(\omega/2)\widehat{\varphi}_{0,\pi,\tau}(\omega/2)\ ,\end{aligned} \tag{3.8}$$

for the standard wavelet, and

$$\begin{aligned}\widehat{\varphi}_{0,\pi,\tau}(\omega) &= \sum_k c_k^0 e^{-ik\omega/2}\widehat{\varphi}_{0,2\pi,\tau}(\omega) \\ &= m_0(\omega/2)\widehat{\varphi}_{0,2\pi,\tau}(\omega)\end{aligned} \tag{3.9}$$

for the alternate case. Since $\widehat{\varphi}_{0,\pi,\tau}(\omega)$ has support on $[-\pi,\pi]$, and $\widehat{\varphi}_{0,\pi,\tau}(\omega/2) = \sqrt{2}\widehat{\varphi}_{0,2\pi,\tau/2}(\omega)$ is positive and continuous on this interval, we may express m as

$$\begin{aligned}m(\omega/2) &= \frac{\widehat{\varphi}_{0,\pi,\tau}(\omega)}{\widehat{\varphi}_{0,2\pi,\tau/2}(\omega)} \\ &= \frac{\varphi_{0,\pi,\tau}(\tau\omega/\pi)}{\varphi_{0,2\pi,\tau/2}(\tau\omega/\pi)}, |\omega| < \pi \ ,\end{aligned} \tag{3.10}$$

and extended periodically for all ω, and similarly for m_0. Thus the coefficients c_k are the Fourier coefficients of the last expression,

$$c_k = \frac{1}{4\pi}\int_{-\pi}^{\pi} \frac{\varphi_{0,\pi,\tau}(\tau\omega/\pi)}{\varphi_{0,2\pi,\tau/2}(\tau\omega/\pi)} e^{ik\omega/2}\, d\omega \ . \tag{3.11}$$

for the scale $m = 0$, which holds for other scales as well. In the case of the alternate approach, the dilation equation changes at each scale and in general we get

$$\widehat{\varphi}_{0,2^m\pi,\tau}(\omega) = \sum_k c_k^m e^{-ik\omega/2}\widehat{\varphi}_{0,2^{m+1}\pi,\tau}(\omega) \ , \tag{3.12}$$

$$c_k^m = \frac{1}{2^{m+2}\pi}\int_{-2^m\pi}^{2^m\pi} \frac{\varphi_{0,2^m\pi,\tau}(\tau\omega/\pi)}{\varphi_{0,2^{m+1}\pi,\tau}(\tau\omega/2\pi)} e^{ik\omega/2}\, d\omega \ . \tag{3.13}$$

Notice that the coefficients are in l^2 but the Fourier series do not converge uniformly since the Fourier transform of the PSWF is not continuous.

3.3 Mother Wavelet

Many choices are possible for the mother wavelet. It should be orthogonal to V_0, should belong to V_1, and its integer translates together with those of the scaling function should be a basis of V_1. These requirements can be achieved in various ways. In the Fourier transform domain our potential mother wavelet ψ, in order to belong to V_1, must have the form for either of the two approaches

$$\widehat{\psi}(\omega) = m_1(\omega/2)\widehat{\phi}_1(\omega) \tag{3.14}$$

where m_1 is a 2π periodic function and ϕ_1 is either of the two PSWFs in (3.7). If it is to be orthogonal to V_0 it must have the property that $\widehat{\psi}(\omega)$ must be orthogonal to $\widehat{\varphi}_{0,\pi,\tau}(\omega)e^{i\omega n}$ for all integers n. But then it must be zero on $(-\pi,\pi)$. The final property is that its integer translates be a basis of the orthogonal complement of V_0 in V_1.

The easiest way of attaining these requirements would be to use the standard wavelet approach in which

$$m_1(\omega/2) = e^{-i\omega/2}\overline{m_0(\omega/2+\pi)} \ .$$

But this is by no means the only possibility. We could even choose $\widehat{\psi}$ to generate an orthornormal sequence by requiring it to have support in $[-2\pi, -\pi] \cup [\pi, 2\pi]$ and satisfy

$$\int e^{in\omega} \left|\widehat{\psi}(\omega)\right|^2 d\omega = 0, n \neq 0 .$$

Rather than either of these definitions we shall use one related to the maximization problem associated with the PSWFs. Both the standard and the alternate approach lead to similar mother wavelets, but in the latter case it depends on the scale chosen. We shall denote the functions resulting from the alternate approach *semi − wavelets* in order to distinguish them from the usual wavelets with a fixed dilation equation at all scales.

Definition 1. The PS mother semi-wavelet at the scale m is given by

$$\psi_m(t) := \cos\left(3\pi 2^{m-1} t\right) \varphi_{0,2^{m-1}\pi,\tau}(t) , \tag{3.15}$$

where the PS father semi-wavelet at scale m is denoted by

$$\phi_m(t) := \varphi_{0,2^m\pi,\tau}(t) , \tag{3.16}$$

for $m = 0, \pm 1, \pm 2, \cdots$. The PS mother wavelet is given by

$$\psi(t) := \cos(3\pi/2t)\varphi_{0,\pi/2,\tau/2}(t) , \tag{3.17}$$

where the PS father wavelet is denoted by

$$\phi(t) := \varphi_{0,\pi,\tau}(t) .$$

The function which maximizes the integral $\int_{-\tau}^{\tau} |f(t)|^2 dt/||f||^2$ given that its Fourier transform has support in $[\pi, 2\pi]$ is the inverse Fourier transform of the transformed PSWF $\widehat{\varphi}_{0,\pi/2,\tau}(\omega - 3\pi/2)$. Similarly the one with support in $[-2\pi, -\pi]$ is $\widehat{\varphi}_{0,\pi/2,\tau}(\omega + 3\pi/2)$. Our mother semi-wavelet has been taken to be the average of these two functions. In the time domain this becomes

$$\psi_0(t) := \cos\left(\frac{3\pi}{2} t\right) \varphi_{0,\pi/2,\tau}(t) .$$

Similar calculations are possible at the other scales as well to obtain the formula in the definition. A father semi-wavelet and its associated mother semi-wavelet pair is shown in Figure 4 and Figure 5 below.

Then the dilation equation for the mother semi-wavelet, at scale $m = 0$, has the form similar to (3.7) given by

$$\psi_0(t) = \sum_k d_k^0 \phi_1(t - k/2) \tag{3.18}$$

in the time domain and

$$\widehat{\psi}_0(\omega) = \sum_k d_k^0 e^{-ik\omega/2} \widehat{\phi}_1(\omega)$$

in the frequency domain. Again the coefficients are given by a formula analogous to (3.12) and similar calculations are possible at the other scales.

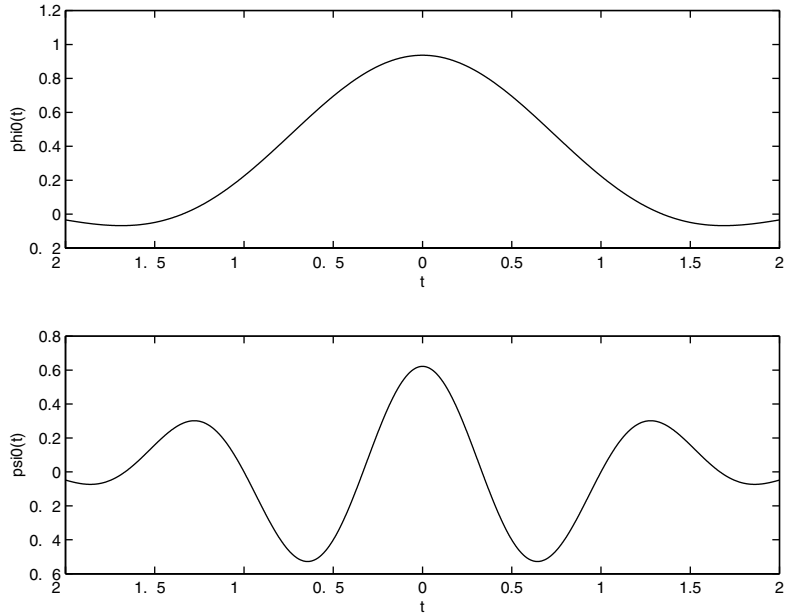

FIGURE 4 A pair of father semi-wavelet $\phi_0(t) = \varphi_{0,\pi,1}(t)$ and its associated mother semi-wavelet $\psi_0(t)$ as defined in (3.15) in the time domain.

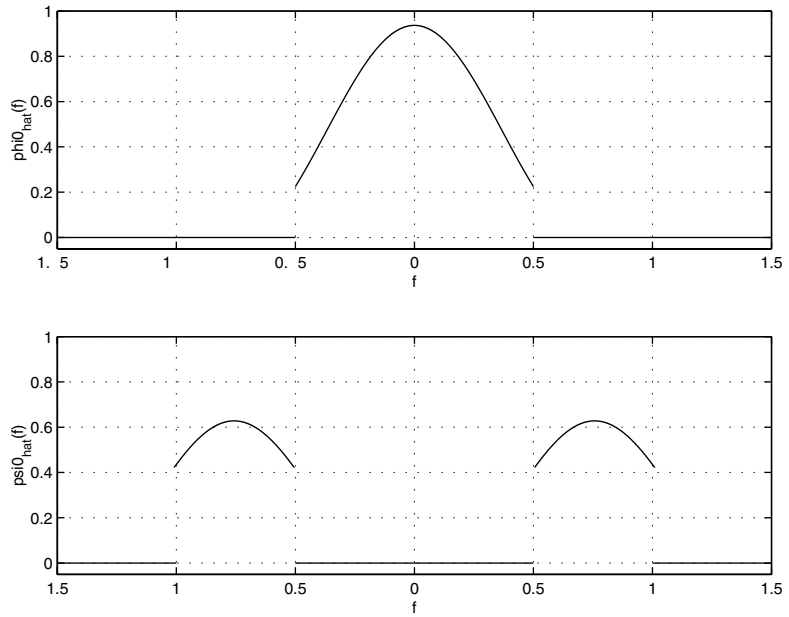

FIGURE 5 The semi-wavelets of Figure 4 $\widehat{\phi}_0(\omega)$ and $\widehat{\psi}_0(\omega)$ in the frequency domain.

As a summary, we state the following theorem:

Theorem 1.

Let $\{\phi_m\}$ *and* $\{\psi_m\}$ *be given by* (3.16) *and* (3.15)*, respectively, let* $V_m = B_{2^m\pi}$ *and let* W_m *be the orthogonal complement of* V_m *in* V_{m+1}*; then* $\{\phi_m(t - 2^{-m}n)\}_{n\in\mathbb{Z}}$ *is a Riesz basis of* V_m *and* $\{\psi_m(t - 2^{-m}n)\}_{n\in\mathbb{Z}}$ *is a Riesz basis of* W_m*.*

The proof of both of these assertions is based on (3.1) and uses the fact that the Fourier transform doesn't vanish on the support of $\{\widehat{\phi}_m\}$ and $\{\widehat{\psi}_m\}$.

For the usual wavelets, we have used the analogous formula for the mother wavelet rather than the standard expression. It is

$$\psi(t) := \cos\left(\frac{3\pi}{2}t\right)\varphi_{0,\pi/2,\tau/2}(t)\ ,$$

but can be reduced to the usual dilation equation by observing that this function belongs to V_1 and hence can be expressed as an infinite linear combination of $\{\phi(2t - k)\}$.

4. Approximation by PS Semi-Wavelet Series

The approximation of a function in $L^2(\mathbb{R})$ by function in V_m is given by a series of the form

$$\sum_k b_k^m \phi_m\left(t - 2^{-m}k\right)\ , \tag{4.1}$$

where the coefficients may be obtained either from the dual Riesz basis or by sampling. In the former case, the result is the projection f_m of a function f onto V_m, while in the latter the result is locally a positive approximation.

The dual Riesz basis is given in terms of its Fourier transform as

$$\begin{aligned}\widehat{\widetilde{\phi}}_m(\omega) &:= \frac{\widehat{\phi}_m(\omega)}{2^{m+1}\pi\sum_k\left|\widehat{\phi}_m\left(\omega - 2^{m+1}\pi k\right)\right|^2} \\ &= \frac{\chi_{2^m\pi}(\omega)}{2^{m+1}\pi\widehat{\phi}_m(\omega)}\end{aligned} \tag{4.2}$$

since $\widehat{\phi}_m$ has support on $[-2^m\pi, 2^m\pi]$ and is positive there. Hence the coefficients for the projection are

$$b_k^m = \int_{-\infty}^{\infty} f(t)\widetilde{\phi}_m\left(t - 2^{-m}k\right)\,dt\ . \tag{4.3}$$

The kernel of this projection is given

$$q_m(x,t) = \sum_k \phi_m\left(x - 2^{-m}k\right)\widetilde{\phi}_m\left(t - 2^{-m}k\right)\ , \tag{4.4}$$

i.e.,

$$f_m(x) = \int_{-\infty}^{\infty} f(t)q_m(x,t)\,dt\ .$$

By taking Fourier transforms of $q_m(x,t)$ in both x and t in the sense of distributions, we obtain

$$\begin{aligned} \widehat{q}_m(\omega,\xi) &= 2\pi\widehat{\widetilde{\phi}_m}(\xi)\widehat{\phi}_m(\omega)\delta\left(2^m(\omega-\xi)\right) \\ &= 2\pi\,\chi_{2^m\pi}(\omega)\delta(\omega-\xi)\,, \end{aligned} \tag{4.5}$$

where upon by taking the inverse Fourier transform again we obtain the familiar sinc function,

$$q_m(x,t) = \frac{\sin 2^m\pi(x-t)}{\pi(x-t)}\,. \tag{4.6}$$

Theorem 2.

Let $f \in H^p$, the Sobolev space, for $p > 0$, let the approximation f_m to f be given by a series of the form (4.1) *where the coefficients are given by* (4.4)*; then the rate of convergence is*

$$||f_m - f|| = O\left(2^{-mp}\right)\,.$$

The proof is based on using the square of the L^2 norm in the transformed domain,

$$\begin{aligned} ||f_m - f||^2 &= \frac{1}{2\pi}\left\|\widehat{f}_m - \widehat{f}\right\|^2 \\ &= \frac{1}{2\pi}\int_{-\infty}^{\infty}\left|\frac{1}{2\pi}\int_{-\infty}^{\infty}\widehat{q}_m(\omega,\xi)\,\widehat{f}(\xi)\,d\xi - \widehat{f}(\omega)\right|^2 d\omega \\ &= \frac{1}{2\pi}\int_{-\infty}^{\infty}\left|\left(\chi_{2^m\pi}(\omega)-1\right)\widehat{f}(\omega)\right|^2 d\omega \\ &= \frac{1}{2\pi}\left\{\int_{2^m\pi}^{\infty}+\int_{-\infty}^{-2^m\pi}\right\}\left|\widehat{f}(\omega)\right|^2 d\omega \\ &= \frac{1}{2\pi}\left\{\int_{2^m\pi}^{\infty}+\int_{-\infty}^{-2^m\pi}\right\}\left|\widehat{f}(\omega)\right|^2\frac{\left(\omega^2+1\right)^p}{\left(\omega^2+1\right)^p}\,d\omega \\ &\le \frac{2}{2\pi}\int_{-\infty}^{\infty}\left|\widehat{f}(\omega)\right|^2\frac{\left(\omega^2+1\right)^p}{\left((2^m\pi)^2+1\right)^p}\,d\omega \\ &= O\left(2^{-2mp}\right)\,, \end{aligned} \tag{4.7}$$

which gives our conclusion.

If the coefficients are given by the sampled values of the function, then the convergence may not be so rapid, but has other nice properties. The approximation in V_m is now given by the hybrid series

$$f_m^s(t) = \sum_k f\left(2^{-m}k\right)\frac{\phi_m\left(t-2^{-m}k\right)}{2^m\widehat{\phi}_m(0)}\,. \tag{4.8}$$

This may again be expressed in terms of a kernel as

$$f_m^s(x) = \int f(t)\,K_m(x,t)\,dt$$

where

$$K_m(x,t) = \sum_k \frac{\phi_m\left(x - 2^{-m}k\right)}{2^m \widehat{\phi}_m(0)} \delta\left(t - 2^{-m}k\right) . \tag{4.9}$$

Theorem 3.

Let $f \in H^p$, the Sobolev space, for $p > 2$, let the approximation f_m^s to f be given by a series of the form (4.8)*; then the rate of convergence is*

$$||f_m - f|| = O\left(2^{-m(p-2)}\right) .$$

The proof involves first obtaining some properties of the kernel $K_m(x,t)$, which we obtain by comparing it to the previous kernel $q_m(x,t)$. The difference between the two lies in the replacement of the dual function $\widetilde{\phi}_m$ by $\delta/\widehat{\phi}_m(0)$. The difference of their Fourier transforms is

$$\begin{aligned}
&\widehat{\widetilde{\phi}}_m(\omega) - \widehat{\delta}(\omega)/\widehat{\phi}_m(0) \\
&\quad = \frac{\chi_{2^m\pi}(\omega)}{2^m\widehat{\phi}_m(\omega)} - \frac{1}{2^m\widehat{\phi}_m(0)} \\
&\quad = \sqrt{\frac{\lambda_{0,\pi,\tau}}{2^{m+1}\tau}}\left[\frac{\chi_{2^m\pi}(\omega)}{\phi_m\left(\tau\omega/2^m\pi\right)} - \frac{1}{\phi_m(0)}\right]
\end{aligned}$$

by (2.3). We now take the first two terms of the power series expansion about 0 of the first term in brackets. Since the derivative is zero at 0, we get

$$\begin{aligned}
\frac{1}{\phi_m\left(\tau\omega/2^m\pi\right)} \quad &= \quad \frac{1}{\phi_m(0)} - \frac{\phi_m''(0)}{\phi_m^2(0)}\frac{\left(\tau\omega/2^m\pi\right)^2}{2} \\
&\qquad + O\left(\tau\omega/2^m\right)^3
\end{aligned} \tag{4.10}$$

for $|\omega| < 2^m\pi$. Now we use the fact that ϕ_m satisfies the differential Equation (1.3) to obtain an expression for the derivative

$$\tau^2\phi_m''(0) = \mu_0\phi_m(0)$$

where $\mu_{0,\sigma,\tau}$ is the eigenvalue of the differential operator. This eigenvalue has been extensively studied and has been shown Bouwkamp [2] to satisfy

$$\mu_{0,\sigma,\tau} = -\frac{1}{3}\left(2^m\pi\tau\right)^2 - \frac{2}{135}\left(2^m\pi\tau\right)^4 + \cdots .$$

If we use only the first term in this expression, as well as in (4.10), then we have approximately

$$\begin{aligned}
&\frac{1}{\phi_m\left(\tau\omega/2^m\pi\right)} - \frac{1}{\phi_m(0)} \\
&\quad \approx \frac{-\frac{1}{3}\left(2^m\pi\right)^2}{\phi_m(0)}\frac{\left(\tau\omega/2^m\pi\right)^2}{2} = -\frac{(\tau\omega)^2}{6\phi_m(0)} .
\end{aligned} \tag{4.11}$$

We now substitute this into the difference between the two kernels K_m and q_m,

$$\begin{aligned}
&\widehat{K}_m(\omega,\xi) - \widehat{q}_m(\omega,\xi) \\
&\quad = \left\{\frac{1}{\widehat{\phi}_m(0)} - \frac{1}{\widehat{\phi}_m(\omega)}\right\}\widehat{\phi}_m(\omega)2\pi\,\chi_{2^m\pi}(\omega)\delta(\omega-\xi) \\
&\quad \approx \frac{(\tau\omega)^2}{6\phi_m(0)}\phi_m\left(\tau\omega/2^m\pi\right)2\pi\,\chi_{2^m\pi}(\omega)\delta(\omega-\xi) .
\end{aligned} \tag{4.12}$$

Hence the difference between our two approximations is

$$\begin{aligned}
&\left\| \widehat{f}_m - \widehat{f}_m^s \right\|^2 \\
&= \int_{-\infty}^{\infty} \left| \frac{1}{2\pi} \int_{-\infty}^{\infty} \left[\widehat{q}_m(\omega, \xi) - \widehat{K}_m(\omega, \xi) \right] \widehat{f}(\xi)\, d\xi \right|^2 d\omega \\
&\approx \int_{-\infty}^{\infty} \left| \frac{1}{2\pi} \int_{-\infty}^{\infty} \left[\frac{(\tau\omega)^2}{6\phi_m(0)} \phi_m\left(\tau\omega/2^m\pi\right) 2\pi\, \chi_{2^m\pi}(\omega)\delta(\omega - \xi) \right] \widehat{f}(\xi)\, d\xi \right|^2 d\omega \\
&= \int_{-2^m\pi}^{2^m\pi} \left| \frac{(\tau\omega)^2}{6\phi_m(0)} \phi_m\left(\tau\omega/2^m\pi\right) \widehat{f}(\omega) \right|^2 d\omega \\
&\le \int_{-2^m\pi}^{2^m\pi} \left| \frac{(\tau\omega)^2}{6} \widehat{f}(\omega) \right|^2 \frac{\left(\omega^2+1\right)^p}{\left(\omega^2+1\right)^p} d\omega \\
&\le 2\left(\left(2^m\pi\right)^2 + 1 \right)^{2-p} \int_{-\infty}^{\infty} \left| \frac{\tau^2}{6} \widehat{f}(\omega) \right|^2 \left(\omega^2+1\right)^p d\omega\,.
\end{aligned}$$

Since $f \in H^p$ for $p > 2$, this last integral is finite and our conclusion follows since a better rate of convergence holds for f_m.

Although the rate of convergence for the hybrid series is slower than for the projection series, the former has other nice properties that may make it more desirable. One is clear: integration is avoided in the calculations of the coefficients. The other is useful, particularly in image approximations: there is no Gibbs phenomenon (overshoots at jump discontinuity). This happens because the kernel is locally positive.

Lemma 1.

Let $K_m(x,t)$ be the kernel given by (4.9)*, let $B < \tau$, then $K_m(x,t) \ge 0$ for $|t| < B$, $|x| < \tau - B$.*

Since $\delta(t - n2^{-m}) = 0$ for $|n2^{-m}| > B$, whenever $|t| < B$, it follows that the expression for K_m is given by a finite sum

$$K_m(x,t) = \sum_{k=-2^m B}^{2^m B} \frac{\phi_m\left(x - 2^{-m}k\right)}{2^m \widehat{\phi}_m(0)} \delta\left(t - 2^{-m}k\right), \; |t| < B\,.$$

But we know that ϕ_m is positive on the interval $[-\tau, \tau]$, and since $x - 2^{-m}k$ lies in this interval when $|x| < \tau - B$, this sum is composed of a finite number of positive distributions and hence is positive (in the sense of distributions).

Corollary 1.

Let f be a piecewise continuous function with a jump discontinuity at 0 *and with support in the interval $[-B, B]$; then f_m^s does not exhibit Gibbs phenomenon in a neighborhood of* 0.

It should be observed that neither the standard wavelet basis of this MRA based on the sinc function nor our new PS wavelet basis leads to a positive kernel of the type shown to exist for our PS semi-wavelet basis. Hence we should expect to observe Gibbs phenomenon for these two other cases.

5. Numerical Examples

In this section we use a standardization that is common in the literature. Rather than use a general concentration interval $[-\tau, \tau]$, we assume our PSWFs to be concentrated on the unit interval $[-1, 1]$. This is really no restriction since we could have changed variables to get this interval by taking our functions to be $2^m\pi\tau$-bandlimited, and then using the formula in (2.6). Rather, since m is allowed to range over all integers, we shall continue to use V_m to denote the space of $2^m\pi$-bandlimited functions.

We now present several examples in this section. We should like to point out that the examples here are purely illustrative. The function in the first example belongs to all Sobolev spaces H^p for all $p > 0$, but is not bandlimited; the function in the second example belongs to the Sobolev space H^3 and has compact support in time domain; the third example discusses a function which has a jump discontinuity at zero and also has compact support. In all cases, we shall compare the approximation for the three different MRA consisting of

(1) the standard Shannon wavelet series defined as:

$$\begin{aligned} f_m^1(t) &:= \sum_{n=-\infty}^{\infty} f\left(n2^{-m}\right) S\left(2^m t - n\right) \\ &\approx \sum_{n=-N}^{N} f\left(n2^{-m}\right) S\left(2^m t - n\right) := f_{m,N}^1(t) \end{aligned} \tag{5.1}$$

where S is the sinc function $S(t) = \sin \pi t/\pi t$.

(2) the PS wavelet series, defined as

$$\begin{aligned} f_m^2(t) &:= \sum_{n=-\infty}^{\infty} a_n^m \phi\left(2^m t - n\right) \\ &= \sum_{n=-\infty}^{\infty} a_n^m \varphi_{0,2^m\pi,2^{-m}\tau}\left(t - n2^{-m}\right) , \\ &\approx \sum_{n=-N}^{N} f\left(n2^{-m}\right) \varphi_{0,2^m\pi,2^{-m}\tau}\left(t - n2^{-m}\right) \\ &= C \sum_{n=-N}^{N} f\left(n2^{-m}\right) \varphi_{0,\pi,\tau}\left(2^m t - n\right) := f_{m,N}^2(t) , \end{aligned} \tag{5.2}$$

where $C = \frac{1}{\phi_{0,\pi,\tau}(0)}\sqrt{2^{-1}\lambda_{0,\pi,\tau}}$, and

(3) the PS semi-wavelet series, defined as

$$
\begin{aligned}
f_m^3(t) &:= \sum_{n=-\infty}^{\infty} b_n^m \phi_m\left(t - n2^{-m}\right) \qquad (5.3)\\
&= \sum_{n=-\infty}^{\infty} f\left(n2^{-m}\right) \frac{\varphi_{0,2^m\pi,\tau}\left(t - n2^{-m}\right)}{2^m \widehat{\phi}_m(0)}\\
&\approx \sum_{n=-N}^{N} C_m f\left(n2^{-m}\right) \varphi_{0,2^m\pi,\tau}\left(t - n2^{-m}\right) := f_{m,N}^3(t)\ ,
\end{aligned}
$$

where $C_m = \frac{1}{\phi_{m,2^m\pi,\tau}(0)}\sqrt{2^{m-1}\lambda_{0,2^m\pi,\tau}}$.

Example 1. The Gaussian kernel defined as

$$G(t) = \frac{1}{\sqrt{2\pi}} e^{-\frac{t^2}{2}},\ t \in R \qquad (5.4)$$

is analytic and both the function and its Fourier transform decay exponentially. Thus it belongs to every Sobolev space, but is not bandlimited and thus cannot be represented exactly by any of our wavelet series at a fixed scale m. However they should converge to it rather rapidly as $m \to \infty$. Figure 6 shows the Shannon series [$G_{m,N}^1$, using (5.1)],

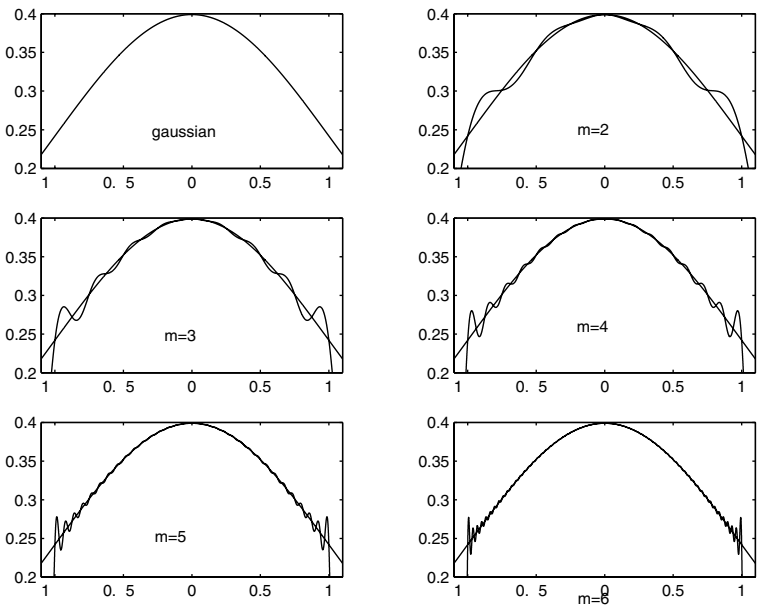

FIGURE 6 The Gaussian kernel $G(t)$, its approximation using Shannon scaling expansion, $G_{m,N}^1(t)$ at different scales, $m = 2, 3, 4, 5, 6$, series truncated to $2N + 1$ terms, $N = 2^m$.

Figure 7 shows PS wavelet series ($G_{m,N}^2$, using (5.2) and Figure 8 shows PS semi-wavelet approximation [$G_{m,N}^3$, using (5.3)] at different resolution level m. Notice that each series has to be truncated to finite terms, here we have used $2N+1$, $N = 2^m$ terms. This is equivalent to

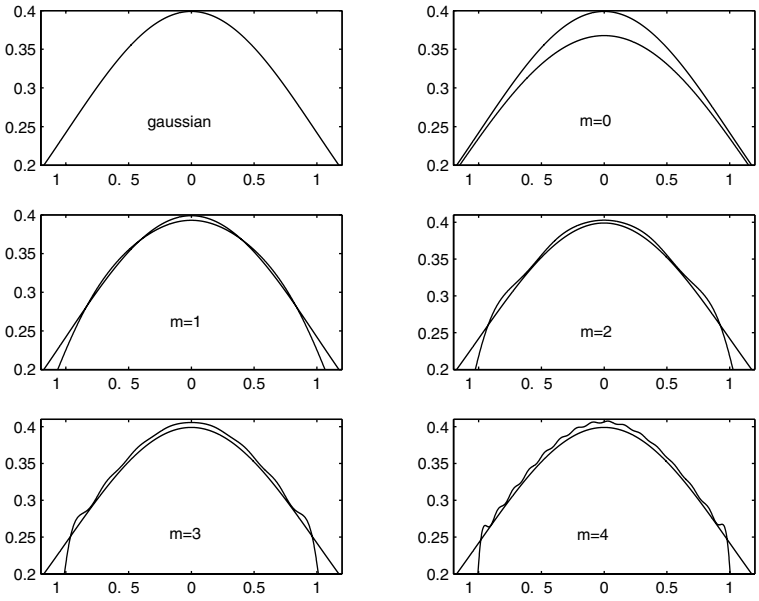

FIGURE 7 $G(t)$ and its PS wavelet approximation $G^2_{m,N}(t)$ at different scales, $m = 0, 1, 2, 3, 4$, series truncated to $2N + 1$ terms, $N = 2^m$.

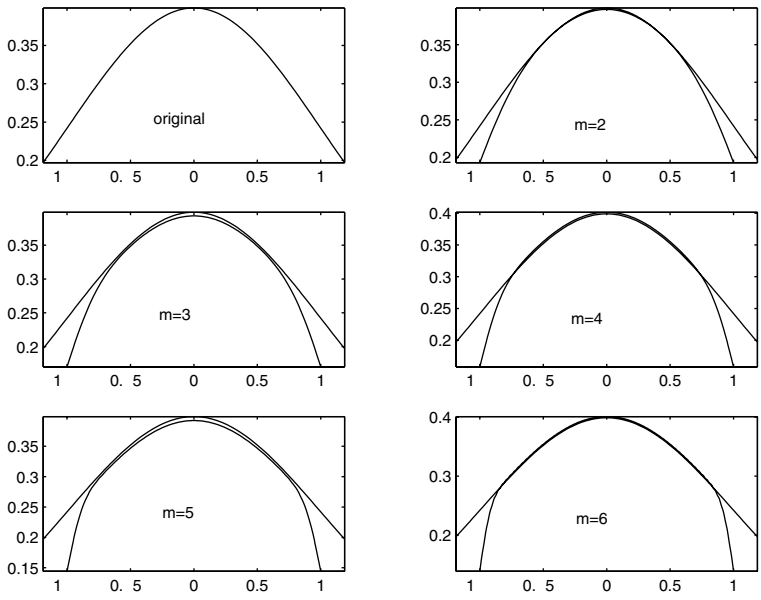

FIGURE 8 $G(t)$ and its PS semi-wavelet approximation $G^3_{m,N}(t)$ at different scales, $m = 2, 3, 4, 5, 6$, series truncated to $2N + 1$ terms, $N = 2^m$.

truncating the function at $|t| > 1$. This truncation results in an overshoot in neighborhoods of $t = \pm 1$ (Gibbs Phenomenon) for both $G^1_{m,N}$, and $G^2_{m,N}$ which doesn't disappear when higher values of m are used in the approximation. However the approximation given by $G^3_{m,N}$ does not show Gibbs phenomenon and has a smoother approximation near these points.

Example 2. The function F given by the formula

$$F(t) = \left\{ \begin{array}{ll} \left(1-t^2\right)^3, & |t| < 1 \\ 0, & |t| \geq 1 \end{array} \right\} \tag{5.5}$$

belongs to the Sobolev space H^3 and has support on the interval [-1,1]. Its Fourier transform converges fairly slowly and we would not expect any of our three series to converge to it very rapidly. In fact, by Theorem 3, the convergence rate in this case is $O(2^{-m})$. $F^1_{m,N}$, $F^2_{m,N}$, and $F^3_{m,N}$ are shown in Figure 9, Figure 10 and Figure 11, respectively. Notice that, in this example and the example follows, the given functions are compactly supported. Therefore, on a finite interval, the series (5.1), (5.2), and (5.3) consists of finite number of terms with exact partial sums whenever $N \geq 2^m$. Since the Shannon series (5.1) converges more rapidly than the other two as $m \to \infty$, and since there is no discontinuity due to truncation, we expect it to represent the function better as indeed it appears to in these three figures.

Example 3. The function used to study Gibbs phenomenon in the case of Fourier series is the saw-tooth wave

$$H(t) = \mathrm{sgn}(t) - t, \ 0 < |t| < 1, 0, \ \text{otherwise.} \tag{5.6}$$

This function can also be used to study Gibbs phenomenon for approximations by wavelets [25]. It is continuous except for a jump of 2 at $t = 0$ and again has support on the interval $[-1, 1]$.

Since $S(t)$ has very poor time localization, we expect both $H^2_{m,N}$ and $H^3_{m,N}$ to represent a function concentrated on $[-\tau, \tau]$ better than $H^1_{m,N}$. We have seen that the convergence kernel in the third case is locally positive, while in the first two cases this is not true. Thus we would expect both to exhibit Gibbs phenomenon but $H^3_{m,N}$ to avoid it. Graphs of the saw-tooth wave function and its approximation by the Shannon series, PS wavelet series and PS semi-wavelets are shown in Figure 12, Figure 13, and Figure 14, respectively. We observe that the graph of the sampling series of the saw-tooth wave function does show "ripples" around origin arising from Gibbs phenomenon as expected in Figures 12 and 13. This should be contrasted with Figure 14 where no such ripples appear.

Finally, we observe that when m increase, the number of the sampling points should be increased accordingly. Otherwise, the truncation error might cause unexpected results especially when the given functions do not decay rapidly. This has been done in all three examples in which a fixed ratio between N and m has been used, that is, $N = 2^m$, since we are mainly interested in aliasing error rather than truncation error. In the case of Examples 2 and 3, this has eliminated the truncation error.

6. Concluding Remarks

Two multiscale systems based on translates of the PSWFs have been constructed. One is a wavelet system which however has decreasing intervals of concentration as the

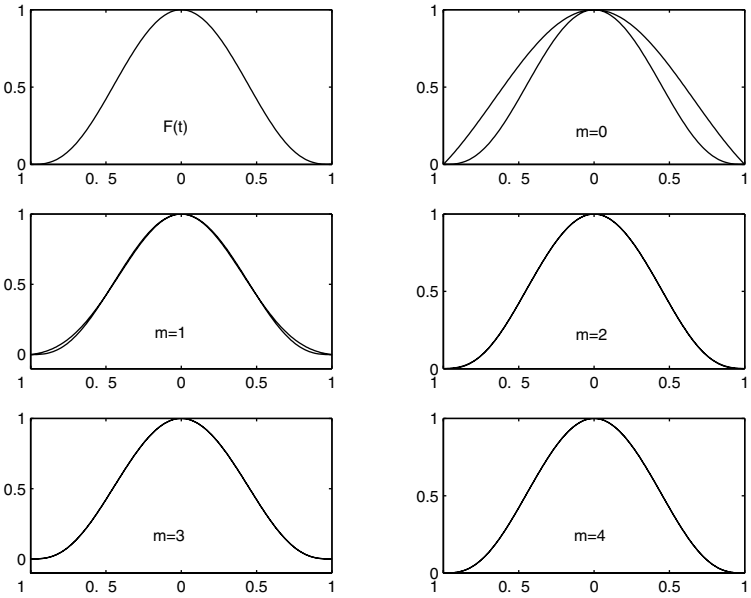

FIGURE 9 $F(t)$ and its Shannon wavelet approximation $F^1_{m,N}(t)$ at different scales, $m = 0, 1, 2, 3, 4$.

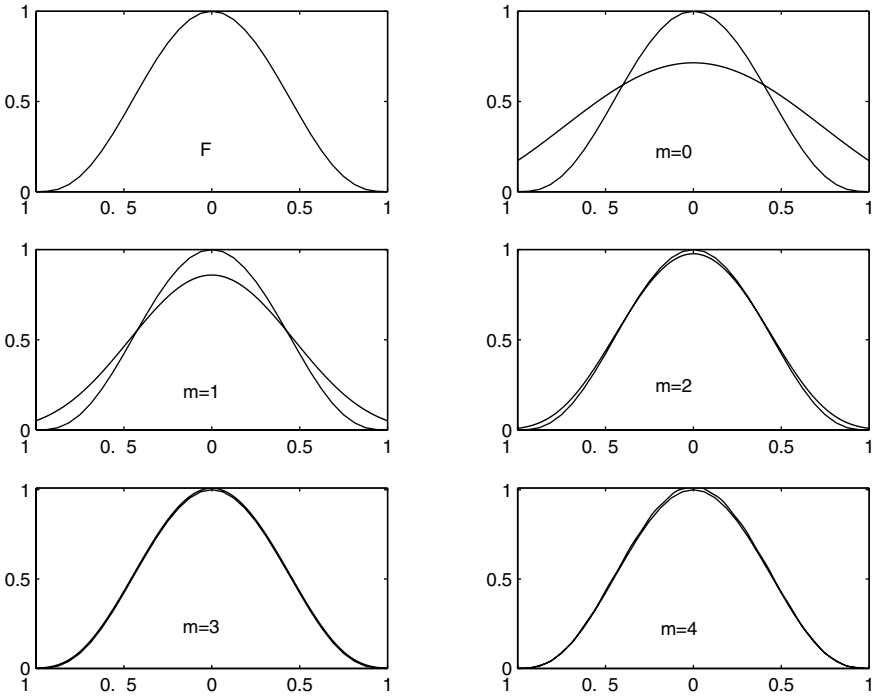

FIGURE 10 $F(t)$ and its PS wavelet approximation $F^2_{m,N}(t)$ at different scales, $m = 0, 1, 2, 3, 4$.

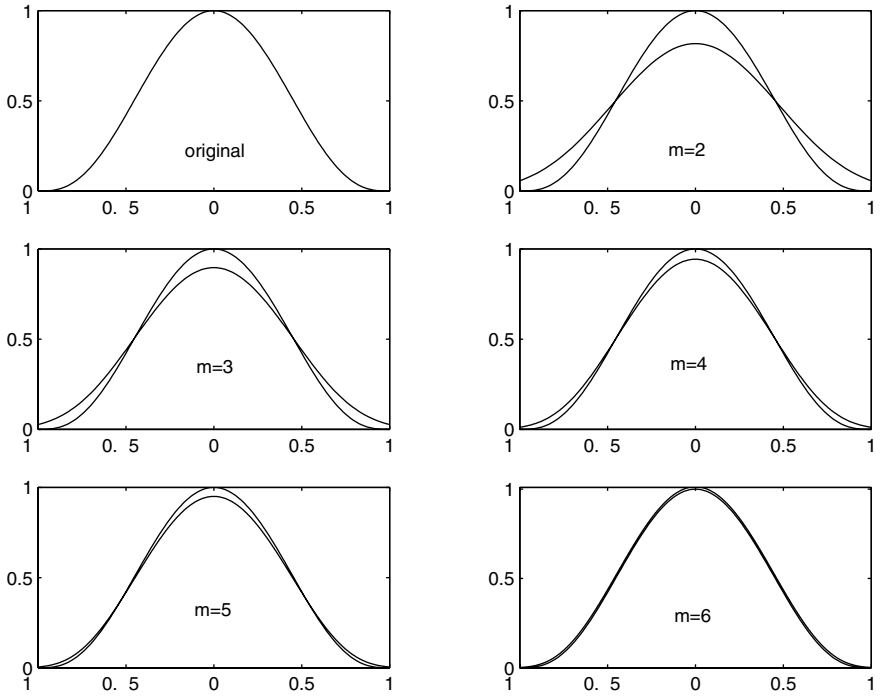

FIGURE 11 $F(t)$ and its PS semi-wavelet approximation $F^3_{m,N}(t)$ at different scales, $m = 2, 3, 4, 5, 6$.

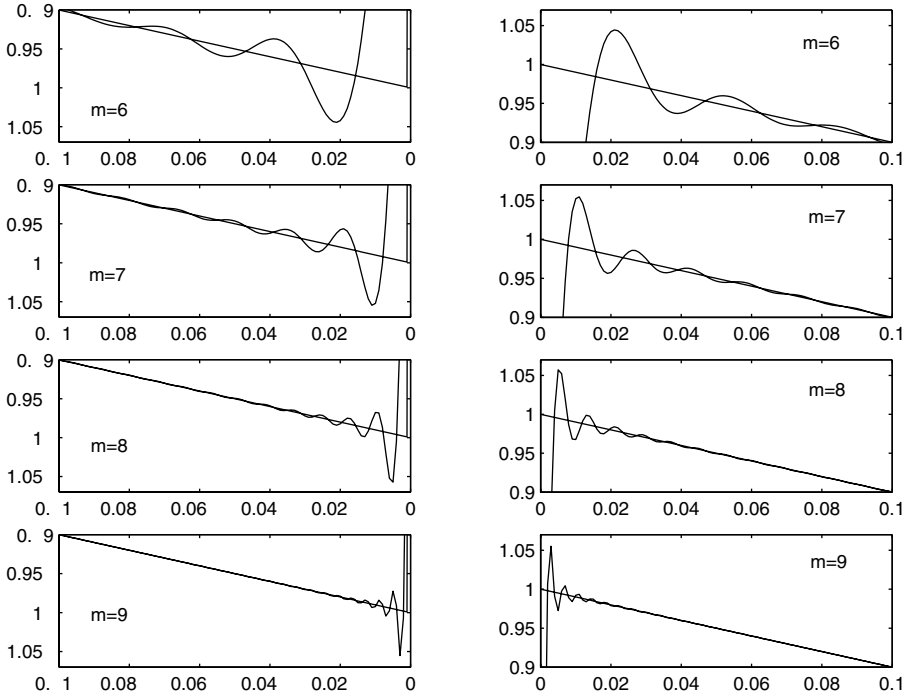

FIGURE 12 $H(t)$ and its Shannon wavelet approximation $H^1_{m,N}(t)$ at different scales, $m = 2, 3, 4, 5, 6$, on both sides of discontinuity.

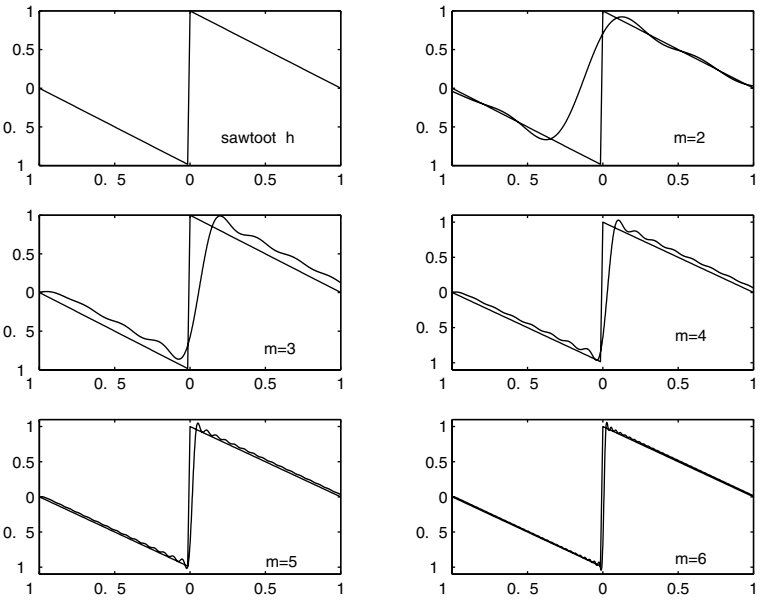

FIGURE 13 $H(t)$ and its PS wavelet approximation $H^2_{m,N}(t)$ at different scales, $m = 0, 1, 2, 3, 4$.

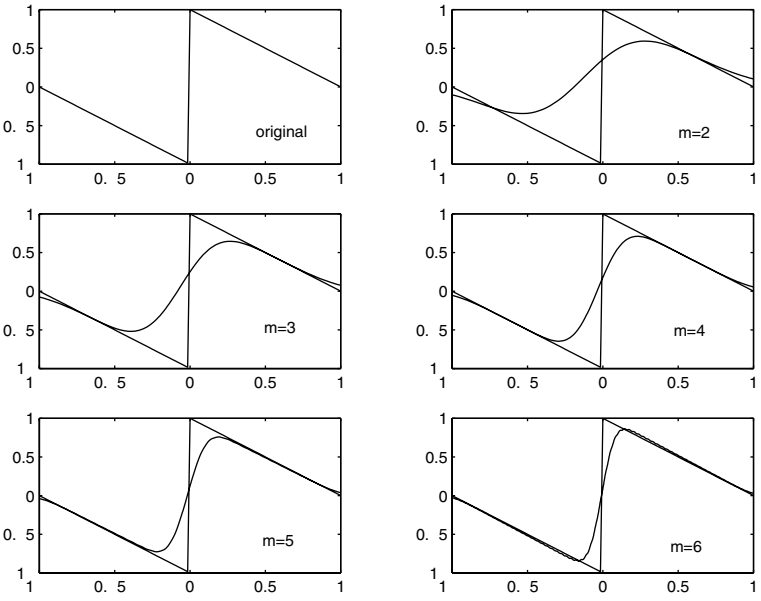

FIGURE 14 $H(t)$ and its PS semi-wavelet approximation $H^3_{m,N}(t)$ at different scales, $m = 2, 3, 4, 5, 6$.

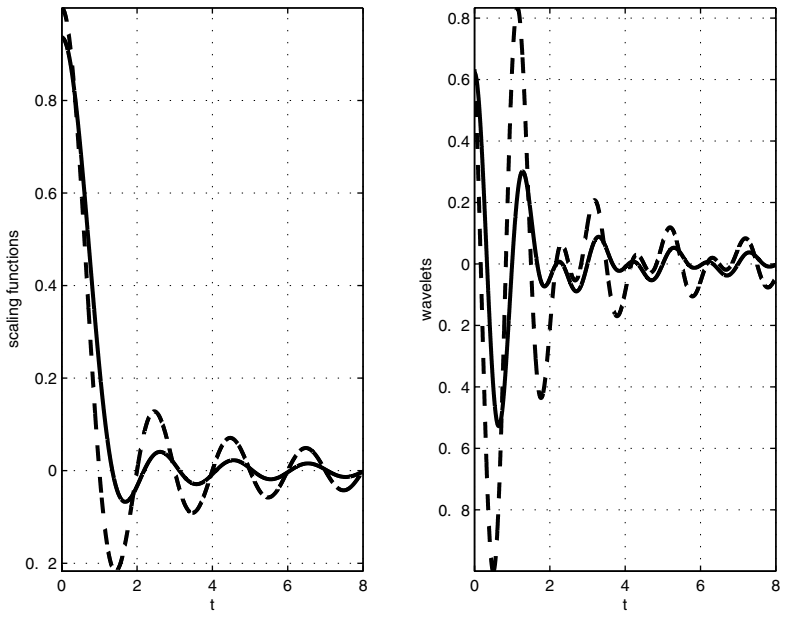

FIGURE 15 The scaling function (left) and mother wavelet (right) of the PS semi-wavelet (solid line) and the Shannon wavelet (dotted line) at scale $m = 0$.

scale increases. The second system, with a structure similar to that of wavelets, preserves the optimized energy concentration intervals inherited from PSWFs, at different scales. Approximation properties are proved theoretically and demonstrated by using numerical examples.

We should like to remark here, except when the given function is compactly supported in the time domain, all of above series (5.1) to (5.3) have to be truncated. The truncation error depends on the decay rate of the given function and the bases. While the asymptotic decay rate of the Shannon basis is exactly the same as that of the wavelets based on PSWFs as $t \to \infty$, the total energy outside of a finite interval is much smaller for the latter. This is demonstrated in Figure 15, where plots of both the scaling functions and mother wavelets in the two cases are shown.

We also point out that the approximations considered here are based only on series in the father wavelet (scaling function) and not on series in the mother wavelet. These latter are needed for thresholding methods which we have not considered in this article. These methods as well as potential applications in some areas such as digital filter design as well as a multiscale algorithm for the numerical implementation are under our further investigation.

Acknowledgments

The second author was partially supported by Professor Naoki Saito's grant ONR YIP N00014-00-1-0469 while completing this article. She is also grateful for the research leave granted by Ohio University.

References

[1] Beylkin, G. and Monzon, L. (2000). On generalized Gaussian quadratures for exponentials and their applications, preprint.

[2] Bouwkamp, C.J. (1947). On spheroidal wave functions of order zero, *J. Math. Phys.,* **26**, 79–92.

[3] Daubechies, I. (1992). *Ten Lectures on Wavelets,* SIAM, Philadelphia.

[4] Djokovic, I. and Vaidyanathan, P.P. (1997). Generalized sampling theorems in multiresolution subspaces, *IEEE Trans. Signal Processing,* **45**(3), 583–599.

[5] Higgins, J.R. (1996). *Sampling series in Fourier Analysis and Signal Theory,* Clarendon Press, Oxford.

[6] Grűnbaum, F.A. (1981). Toeplitz matrices commuting with tridiagonal matrices, *J. Linear Alg. and Appl.,* **40**, 25–36.

[7] Jain, K.A. (1989). *Fundamentals of Digital Image Processing,* Englewood Cliffs, NJ, Prentice Hall.

[8] Landau, H.J. and Widom, H. (1980). The eigenvalue distribution of time and frequency limiting, *J. Math. Anal. Appl.,* **77**, 469–481.

[9] Landau, H.J. and Pollak, H.O. (1961). Prolate spheroidal wave functions, Fourier analysis and uncertainty, II, *Bell System Tech. J.,* **40**, 65–84.

[10] Landau, H.J. and Pollak, H.O. (1962). Prolate spheroidal wave functions, Fourier analysis and uncertainty, III, *Bell System Tech. J.,* **41**, 1295–1336.

[11] Landau, H.J. (1967). Sampling, data transmission, and the Nyquist rate, *Proc. IEEE,* **55**, 1701–1706.

[12] Meyer, Y. (1990). *Ondelettes et Opérateurs* I, Herman, Paris.

[13] Nashed, M.Z. and Walter, G.G. (1991). General sampling theorems for functions in reproducing kernel Hilbert spaces, *Math. Control, Signals, Systems,* **4**, 363–390.

[14] Papoulis, A. (1977). *Signal Analysis,* McGraw-Hill, New York.

[15] Rudin, W. (1973). *Functional Analysis,* McGraw-Hill, New York.

[16] Shannon, C.E. (1949). Communication in the presence of noise, *Proc. IRE* **37**, 10–21.

[17] Slepian, D. and Pollak, H.O. (1961). Prolate spheroidal wave functions, Fourier analysis and uncertainty, I, *Bell System Tech. J.,* **40**, 43–64.

[18] Slepian, D. (1964). Prolate spheroidal wave functions, Fourier analysis and uncertainty, IV, *Bell System Tech. J.,* **43**, 3009–3058.

[19] Slepian, D. (1983). Some comments on Fourier analysis, uncertainty,and modeling, *SIAM Review,* **25**, 379–393.

[20] Vaidyanathan, P.P. (2001). Sampling theorems for non-bandlimited signals: Theoretical impact and practical applications, *Proc SAMPTA 2001,* 17–26.

[21] Walter, G.G. (1992). A sampling theorem for wavelet subspaces, *IEEE Trans. Inform. Theory,* **38**, 881–884.

[22] Walter, G.G. (1992). Differential operators which commute with characteristic functions with applications to a lucky accident, *Complex Variables,* **18**, 7–12.

[23] Walter, G.G. and Shen, X. (2002). Positive sampling in wavelet subspaces, *Appl. Comp. Harmonic Anal.,* **12**(1), 150–165.

[24] Walter, G.G. and Shen, X. (2003). Sampling with prolate spheroidal functions, *J. of Sampling Theory in Signal and Image Processing,* **2**(1), 25–52.

[25] Walter, G.G. and Shen, X. (2000). *Wavelets and Other Orthogonal System, 2nd ed.,* CRC Press, Boca Raton, FL.

[26] Xiao, H., Rokhlin, V., and Yarvin, N. (2000/2001). Prolate spheroidal wavefunctions, quadrature and interpolation, Special issue to celebrate Pierre Sabatier's 65th birthday (Montpellier), *Inverse Problems,* **17**(4), 805–838.

[27] Zayed, A. (1993). *Advances in Shannon's Sampling Theory,* CRC Press, Boca Raton, FL.

Received February 14, 2002

Revision received January 02, 2003

Mathematics Department University of Wisconsin-Milwaukee, Milwaukee, WI 53201
e-mail: ggw@csd.uwm.edu

Mathematics Department, Ohio University, Athens, Ohio 45701
e-mail: xashen@math.ucdavis.edu